VARIATIONAL MODELS FOR IMAGE COLORIZATION VIA CHROMATICITY AND BRIGHTNESS DECOMPOSITION

By

Sung Ha Kang

and

Riccardo March

IMA Preprint Series # 2138

(October 2006)

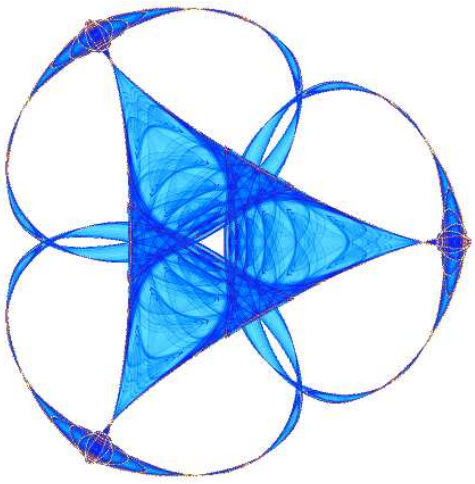

INSTITUTE FOR MATHEMATICS AND ITS APPLICATIONS

UNIVERSITY OF MINNESOTA

400 Lind Hall

207 Church Street S.E.

Minneapolis, Minnesota 55455–0436

Phone: 612-624-6066 Fax: 612-626-7370

URL: http://www.ima.umn.edu

Variational Models for Image Colorization via Chromaticity and Brightness Decomposition

Sung Ha Kang*and Riccardo March†

Abstract

Colorization refers to an image processing task which recovers color of gray scale images when only small regions with color are given. We propose a couple of variational models using chromaticity color component to colorize black and white images. We first consider Total Variation minimizing (TV) colorization which is an extension from TV inpainting to color using chromaticity model. Secondly, we further modify our model to weighted harmonic maps for colorization. This model adds edge information from the brightness data, while it reconstructs smooth color values for each homogeneous region. We introduce penalized versions of the variational models, we analyze their convergence properties, and we present numerical results including extension to texture colorization.

1 Introduction

In this paper we discuss the problem of recovering a color image from a gray scale image and color data given only in small regions. This problem has been considered by Fornasier in [23], where the author introduced various models for the task and connected with inpainting literature. A specific application is considered in [23], which consists in recovering frescoes (paintings) by A. Mantegna in an Italian church which was destroyed during World War II. There are photos of the full frescoes available in black and white, while only few real pieces of frescoes with original colors are remaining. The objective is to reconstruct the original color of the frescoes (image) from few remaining pieces with the original color and full black and white image. In [23], the author used RGB color model with a nonlinear distortion function for fitting the grayscale data, and presented successful numerical results. Some mathematical analysis of the color restoration model of [23] has been presented by Fornasier and March in [24].

This color restoration task is closely related to colorization of black and white images in computer graphics. In [31], the authors notice the neighboring pixels with similar intensities should have similar color, and use non-local fitting term to match the colors. In [39], Sapiro suggests minimizing difference between the gradient of luminance and the gradient of color. The change in color is constrained by the change in luminance, and the method reduces to solving linear or nonlinear Poisson equations. A fast algorithm using weighted distance image blending technique is studied in [49]. The authors utilize Dijkstra's shortest path algorithm for fast computation. More related literature, some using segmented images can be found at [16, 29, 38].

We propose variational colorization models using chromaticity and brightness color model. Color images can be treated in various ways [27]. There are typical linear models such as RGB (Red, Green and Blue channels) and CMY (Cyan, Magenta and Yellow); Luminance separated color systems such as YIQ (Luminance, Hue and Saturation) which is used in standard color TV broadcasting, and YCbCr (Luminance,two color-difference components) widely used for digital video; nonlinear color systems closer to human color perception such as HSV (Hue, Saturation and Value). In more mathematical settings, color images can also be treated as 3-dimensional vectorial functions [8] as well as tensor products of different color components

*Department of Mathematics, University of Kentucky, Lexington, KY 40515, USA (skang@ms.uky.edu)

†Istituto per le Applicazioni del Calcolo, CNR, Viale del Policlinico, 137, 00161 Rome, Italy (r.march@iac.cnr.it)

such as Chromaticity and Brightness (CB). The related literature on different color image models can be found at [11, 30, 36, 40, 43, 44].

In this paper, we use Chromaticity and Brightness (CB) color model. If Ω denotes the image domain, from typical RGB color model,

$$f : \Omega \to \mathbb{R}^3_+ = \{(r, g, b) : r, g, b > 0\},$$

image f is separated into the *brightness component* $B = |f|$, and the *chromaticity component* $C = f/|f| = f/B$, where $|\cdot|$ denotes the Euclidean norm of vectors. In [11], the authors showed that using CB model gives better color control and detail recovery for color image denoising compared to different color settings. For example, it is better to separate chrominance (color information) from the brightness (or luminance) to better control the details of the images. This is consistent with the fact that the essential geometrical information of images is contained in the gray level, as it has been shown in [9]. Therefore, treating brightness separately from the chromaticity can give more flexibility in detail recovery. On the other hand, it is not ideal to separate the chrominance into more than one components. By separating the color components, it unavoidably introduces undesirable art-effects and results in the color which are not close to human vision perception. For example, if chromaticity is separated to Hue and Saturation, since Hue does not have gray as a color, any white (or black) color will have maximum (or minimum) saturation with any random color in Hue. Instead chromaticity is ideal to represent color and it is self-contained as one component representing the chrominance.

The brightness component B is a gray scale image; however, the chromaticity component C stores the color information which takes values on the unit sphere S^2. For this kind of constraints there are various numerical methods introduced to accurately compute non-flat features. Some mathematical analysis on S^N constraints is studied in [25], and numerical methods are explored in [46]. In this paper, we introduce variational colorization models which use a penalty term to deal with S^2 constraint. The penalization method simplifies the computation by avoiding the direct numerical implementation of the constraint. Convergence of solutions of the variational problems with penalty term to solutions of the original problem with S^2 constraint will be shown, as the penalty parameter tends to infinity. In practice, large values of the penalty parameter still yield accurate computed results.

We note that depending on how the gray scale images are given, either as Brightness, Luminance or Value, we can apply our models for each case with simple modification. In the remaining of the paper, we use brightness as a representation of such values, i.e. Brightness, Luminance or Value.

We propose a couple of variational models for colorization. The Total Variation minimizing denoising model by Rudin, Osher, and Fatemi [37] has been extended to various image processing tasks, one of which is TV inpainting method [14]. The colorization task can also be understood as inpainting the colors (as Sapiro's insight [39]). We introduce Total Variation minimizing (TV) colorization using chromaticity and brightness color model. Secondly, we further modify our model using weighted harmonic maps for colorization. This model appropriately adds edge information from the Brightness data, while it reconstructs smooth color values for each homogeneous region. In spirit, this has relations to Mumford-Shah functional for segmentation [34]. The proposed weighted harmonic map functional is flexible in modeling so that it can easily be extended to include texture colorization.

The paper is organized as follows. In section 2, we propose TV colorization using CB model. We show a convergence property of the variational problem with penalty term to the TV colorization model with S^2 constraint, and we present numerical results for TV colorization. In section 3, we propose a functional based on weighted harmonic maps for colorization. We show an analogous convergence property for a penalized version of the model, and we present numerical results including an application to texture colorization.

2 Colorization via Total Variation minimization

In this section, we consider a TV colorization model with chromaticity constraint as a fitting term. We first recall the definition of vector valued functions of bounded variation. Let Ω be a bounded open subset of $\mathbb{R}^n$. We denote the norm on the Banach spaces $L^p(\Omega)$ by $\|\cdot\|_{L^p(\Omega)}$, $1 \le p \le \infty$.

For any $m \in \mathbb{N}$, the space $BV(\Omega;\mathbb{R}^m)$ of functions of bounded variation mapping Ω to $\mathbb{R}^m$ is defined as the set of functions $u \in L^1(\Omega;\mathbb{R}^m)$ such that $\int_\Omega |Du| < +\infty$, where

$$\int_\Omega |Du| = \sup_{\phi\in\Phi} \sum_{i=1}^{m} \int_\Omega u_i \mathrm{div}\phi_i dx,$$

where $u = (u_1, \ldots, u_m)$, $\phi = (\phi_1, \ldots, \phi_m)$, and the supremum is taken on the set of functions

$$\Phi = \left\{ \phi \in C_0^1(\Omega;\mathbb{R}^{m\times n}) : \ |\phi(x)| \leq 1 \text{ for all } x \in \Omega \right\}.$$

Here, and in what follows, the vector norm $|\cdot|$ denotes the Euclidean norm. If $u \in C^1(\Omega;\mathbb{R}^m)$, one can show using integration by parts that

$$\int_\Omega |Du| = \int_\Omega |\nabla u| dx.$$

If $u \in BV(\Omega;\mathbb{R}^m)$, then the partial derivatives of u in the sense of distributions are measures with finite total variation in Ω. If we denote the $m \times n$ matrix of the distributional derivatives by Du (whose entries are denoted by $D_j u_i$), then $\int_\Omega |Du|$ is the total variation of the matrix-valued measure Du. For further information concerning functions of bounded variation, we refer to [1, 26].

In the following, we set $n = 2$, $m = 3$, and Ω denotes the open set $]0,1[\times]0,1[$ of $\mathbb{R}^2$. We denote by S^2 the unit sphere in $\mathbb{R}^3$: $S^2 = \{\xi \in \mathbb{R}^3 : |\xi| = 1\}$. We denote by $BV(\Omega;S^2)$ the set of vector valued functions $u \in BV(\Omega;\mathbb{R}^3)$ such that $u(x) \in S^2$ for almost every $x \in \Omega$.

The set Ω is the image domain and the measurable subset $D \subset \Omega$ denotes the *inpainting domain* where we wish to colorize. Let $D^c = \Omega \setminus D$ be the complement of D in Ω, where the color is given. The vector field $f_o \in L^\infty(D^c;\mathbb{R}^3)$ denotes the color of the given image which is known in the set D^c. The function $B_o \in L^\infty(\Omega)$ denotes the brightness datum which is known everywhere in Ω. The brightness component is such that $B_o(x) \neq 0$ for any $x \in D^c$ and $B_o(x) = |f_o(x)|$ for almost every $x \in D^c$. Then the chromaticity component $C_o = f_o/B_o$ is defined for a.e. $x \in D^c$ and we have $C_o \in L^\infty(D^c;S^2)$.

We consider the following functional depending on chromaticity for TV colorization,

$$E(C) = \int_\Omega |DC| + \lambda \int_{D^c} |C - C_o|^2 dx, \tag{1}$$

where λ denotes a positive weight, and the corresponding minimization problem

$$(\mathcal{P}) \qquad \min\left\{E(C) : C \in BV(\Omega;S^2)\right\}.$$

The first term in the functional E acts as a regularization functional, while the second term requires the unitary vector field C to be close to the given chromaticity data C_o in D^c according to the L^2 distance. The variational problem $(\mathcal{P})$ constitutes a vectorial version of the TV inpainting method considered by Chan and Shen in [14], more precisely for chromaticity. A solution of $(\mathcal{P})$ then represents an extension of the chromaticity data C_o from the subdomain D^c to a vector field C defined in the whole domain Ω. Then, from the given gray image B_o, the colorized image $f \in L^\infty(\Omega;\mathbb{R}^3)$ can be defined by simply setting $f = B_o C$.

Since we use the chromaticity and brightness model for color, we also need to satisfy the $C \in S^2$ constraint. While the functional (1) is convex, the constraint $C(x) \in S^2$ for a.e. $x \in \Omega$ is not convex. Therefore, such a constraint is not trivial to satisfy. A numerical method based on the solution of an unconstrained minimization problem on the entire space of functions has been proposed by Vese and Osher in [46]. In this paper, we consider the following penalized version of the variational problem which consists in the minimization of a nonconvex functional with a convex constraint. For any real number $\alpha > 0$, we consider the functional

$$E_\alpha(C) = \int_\Omega |DC| + \lambda \int_{D^c} |C - C_o|^2 dx + \alpha \int_\Omega \left(1 - |C|\right)^2 dx, \tag{2}$$

and the corresponding minimization problem

$$(\mathcal{P}_\alpha) \qquad \min\left\{E_\alpha(C) : C \in BV(\Omega;\mathbb{R}^3),\ |C(x)| \le 1 \text{ for a.e. } x \in \Omega\right\}.$$

Using this colorization functional, the chromaticity satisfies S^2 constraint as α tends to infinity, while color is inpainted in the domain D by the TV method. In the following subsections, we discuss the convergence properties of minimizers of the penalized variational problems, and present the numerical results of TV colorization.

2.1 Convergence of minimizers for TV colorization with penalty term

In this section, we prove existence of solutions of the variational problem $(\mathcal{P}_\alpha)$ and their convergence, up to subsequences, to solutions of the variational problem $(\mathcal{P})$ as α tends to infinity.

Proposition 1 *For any $\alpha > 0$, there exists a solution to the variational problem $(\mathcal{P}_\alpha)$. Let $\{C_\alpha\}_\alpha \subset BV(\Omega;\mathbb{R}^3)$ be a sequence of functions such that α tends to infinity and C_α solves the variational problem $(\mathcal{P}_\alpha)$ for any $\alpha > 0$. Then there exist a function $C \in BV(\Omega;S^2)$ and a subsequence $\{C_{\alpha_k}\}_k$ such that C_{α_k} converges strongly to C in $L^p(\Omega;\mathbb{R}^3)$ for all $1 \le p < \infty$ as k tends to infinity, and C solves the variational problem $(\mathcal{P})$.*

Proof. *Step 1: Existence of minimizers for fixed α.*

Let $\alpha > 0$ be fixed and let $\{C_h\}_h \subset BV(\Omega;\mathbb{R}^3)$ be a sequence such that, for any $h \in \mathbb{N}$, we have $|C_h(x)| \le 1$ for a.e. $x \in \Omega$ and $E_\alpha(C_h) \le K$, with K a positive constant independent of h. Then we have

$$\int_\Omega |DC_h| \le K, \qquad \|C_h\|_{L^\infty(\Omega)} \le 1,$$

for any h. Then, by using the compactness theorem in BV [26], there exist a function $C \in BV(\Omega;\mathbb{R}^3)$ such that $|C(x)| \le 1$ for a.e. $x \in \Omega$, and a subsequence $\{C_{h_k}\}_k$ such that C_{h_k} converges to C a.e. in Ω, and strongly in $L^p(\Omega;\mathbb{R}^3)$ for all $1 \le p < +\infty$, as k tends to infinity.

Using the Fatou's lemma we have

$$\liminf_{k\to+\infty} \int_{D^c} |C_{h_k} - C_o|^2 dx \ge \int_{D^c} |C - C_o|^2 dx, \qquad \liminf_{k\to+\infty} \int_\Omega \left(1 - |C_{h_k}|\right)^2 dx \ge \int_\Omega \left(1 - |C|\right)^2 dx. \tag{3}$$

Using the lower semicontinuity of the total variation [26] we have

$$\liminf_{k\to+\infty} \int_\Omega |DC_{h_k}| \ge \int_\Omega |DC|. \tag{4}$$

Then, by taking C_h for a minimizing sequence, the existence of a solution for the variational problem $(\mathcal{P}_\alpha)$ follows from the compactness property and by the lower semicontinuity inequalities (3) and (4).

Step 2: Convergence of minimizers when $\alpha \to \infty$.

Let $\{C_\alpha\}_\alpha$ be a sequence such that C_α solves the variational problem $(\mathcal{P}_\alpha)$ for any $\alpha > 0$. Let $C^{(1)}$ denote a constant vector field such that $|C^{(1)}(x)| = 1$ for all $x \in \Omega$. For instance, $C^{(1)}$ can be taken as one of the vectors of the canonical basis of $\mathbb{R}^3$. Then, for any $\alpha > 0$, we have

$$E_\alpha(C_\alpha) \le E_\alpha(C^{(1)}) \le \lambda \int_{D^c} |C^{(1)} - C_o|^2 dx = L,$$

where L is a positive constant independent of α. Then we have

$$\int_\Omega |DC_\alpha| \le L, \qquad \|C_\alpha\|_{L^\infty(\Omega)} \le 1,$$

for any $\alpha > 0$. Then there exist a function $C \in BV(\Omega; \mathbb{R}^3)$ such that $|C(x)| \leq 1$ for a.e. $x \in \Omega$, and a subsequence $\{C_{\alpha_k}\}_k$ such that C_{α_k} converges to C a.e. in Ω, and strongly in $L^p(\Omega; \mathbb{R}^3)$ for all $1 \leq p < +\infty$, as k tends to infinity.

For any $\alpha > 0$, we have

$$\alpha \int_\Omega (1 - |C_\alpha|)^2 \, dx \leq E_\alpha(C_\alpha) \leq L,$$

which implies

$$\lim_{\alpha \to +\infty} \int_\Omega (1 - |C_\alpha|)^2 \, dx = 0,$$

therefore, $|C_\alpha|$ converges to one in $L^2(\Omega)$. Since C_{α_k} converges to C a.e. in Ω, it follows that $|C(x)| = 1$ for a.e. $x \in \Omega$, and $C \in BV(\Omega; S^2)$.

We now show that the function C solves the variational problem $(\mathcal{P})$: for any $\widehat{C} \in BV(\Omega; S^2)$, since $|\widehat{C}(x)| = 1$ for a.e. $x \in \Omega$, we have

$$E(\widehat{C}) = E_\alpha(\widehat{C}) \geq E_\alpha(C_\alpha) \qquad \text{for any } \alpha > 0.$$

Using the Fatou's lemma and the lower semicontinuity of the total variation, as in the proof of Step 1, Eqs. (3) and (4), we have

$$\liminf_{k \to +\infty} E_{\alpha_k}(C_{\alpha_k}) \geq \int_\Omega |DC| + \lambda \int_{D^c} |C - C_o|^2 dx.$$

Then, it follows

$$E(\widehat{C}) \geq \liminf_{k \to +\infty} E_{\alpha_k}(C_{\alpha_k}) \geq \int_\Omega |DC| + \lambda \int_{D^c} |C - C_o|^2 dx = E(C),$$

for any $\widehat{C} \in BV(\Omega; S^2)$. Therefore, C solves the problem $(\mathcal{P})$. $\square$

2.2 Numerical experiments for TV colorization

In this subsection, we present numerical validation of TV colorization method. We use a simple numerical scheme for implementations, which is based on the S^2 penalty method. We first solve the Euler-Lagrange equation of the functional (2), which is formally given by

$$-\nabla \left(\frac{\nabla C}{|\nabla C|} \right) + 2\widehat{\lambda}(C - C_o) + 2\alpha \left(1 - \frac{1}{|C|} \right) C = 0.$$

Here $\widehat{\lambda}$ includes a characteristic function indicating the region for inpainting, i.e.

$$\widehat{\lambda} = \begin{cases} \lambda & \text{for } x \in D^c \\ 0 & \text{for } x \in D \end{cases},$$

therefore, color information is only fitted for given color in region D^c. For numerical implementation, we use the digital TV filter introduced in [13]: we set

$$w^n = \frac{1}{\sqrt{\sum_N (C_N^n - C^n)^2}},$$

where n denotes the iteration step, and N corresponds to four neighborhood of each pixel (i, j), i.e., $N = \{(i-1, j), (i+1, j), (i, j+1), (i, j-1)\}$. Then, C is calculated from

$$C^{n+1} = \frac{\widehat{\lambda} C_o + \sum_N (w^n + w_N^n) C_N^n}{\widehat{\lambda} + \alpha(1 - 1/|C^n|) + \sum_N (w^n + w_N^n)}. \tag{5}$$

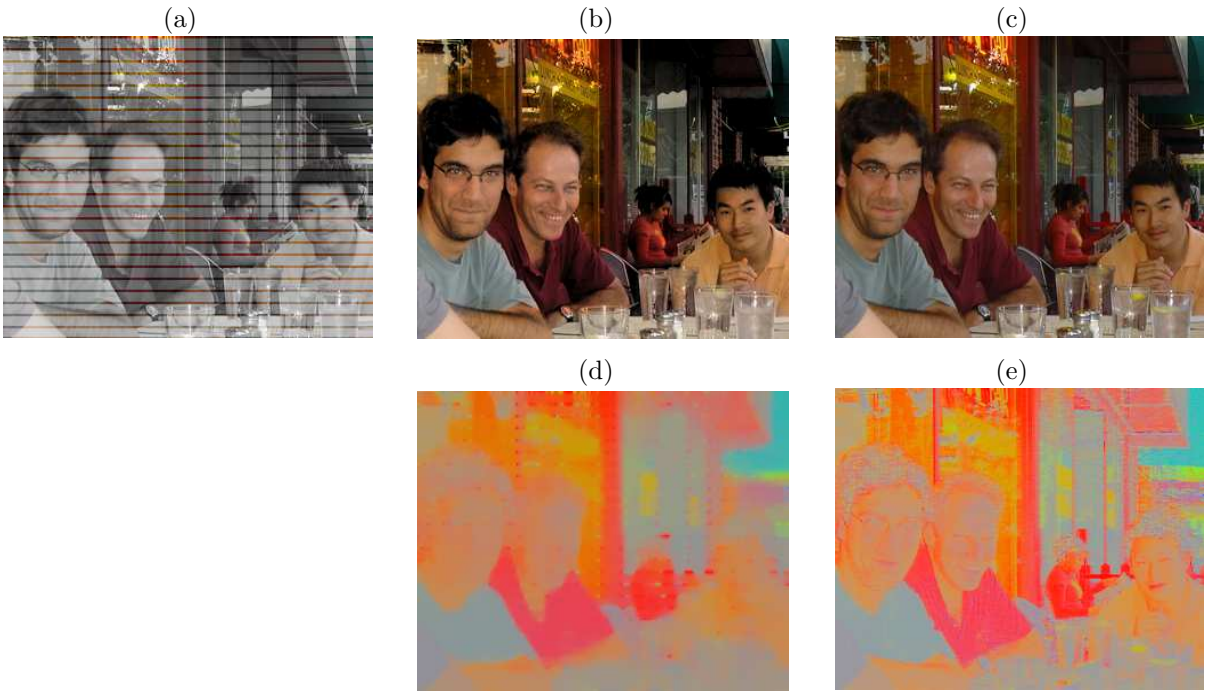

Figure 1: (a) The given image. Thin strips are where the colors are known. (b) TV colorized result. (c) The original image. The second row shows the corresponding chromaticity for each image. The face color of each person, complicated objects such as glasses, as well as the detailed background colors, are well recovered.

After each iteration, C is projected to be $|C(x)| \leq 1$, according to the theory. For our experiments, the image f is in between $[0, 1]$, and $\alpha = 10$ and $\lambda = 10$.

Figure 1 and Figure 2 show numerical results for TV colorization model. From thin strips of given color, the model inpaints the color well and the recovered results are similar to the original color images. The face color of each person is recovered, as well as complicated objects, such as glasses. The complicated background with many fine details and varying colors is clearly recovered. TV colorization is versatile with reasonable computational cost.

This TV colorization method is based on TV inpainting [14] for the colors. Therefore, this inherits the limitations of first order inpainting methods such as [7, 14] (higher order inpainting methods are available to better deal with this situations [6, 12, 15]). Notice from Figure 2 (b), the nose of right seahorse is colored blue, which is the same color as the sky, since this minimizes the total variation. In [10], the error bound for such TV inpainting is studied, and it is shown that the error is bounded by the width of the inpainting domain D. Therefore, TV inpainting method will work well for narrow inpainting domains. In the following section, we present a more flexible colorization model which can colorize larger regions.

3 Colorization via weighted harmonic map

In this section we present a variational model for large domain colorization. This considers cases when only small regions are given with color and large area needs to be colorized. These cases are similar to [23] where the colors are given by pieces of images, or [31, 39, 49] where colors are given by strucks of colors.

We denote by $W^{1,2}(\Omega; \mathbb{R}^m)$ the Sobolev space of functions $u \in L^2(\Omega; \mathbb{R}^m)$ whose first order distributional derivatives all belong to $L^2(\Omega)$. We denote by $W^{1,2}(\Omega; S^2)$ the set of vector valued functions $u \in W^{1,2}(\Omega; \mathbb{R}^3)$

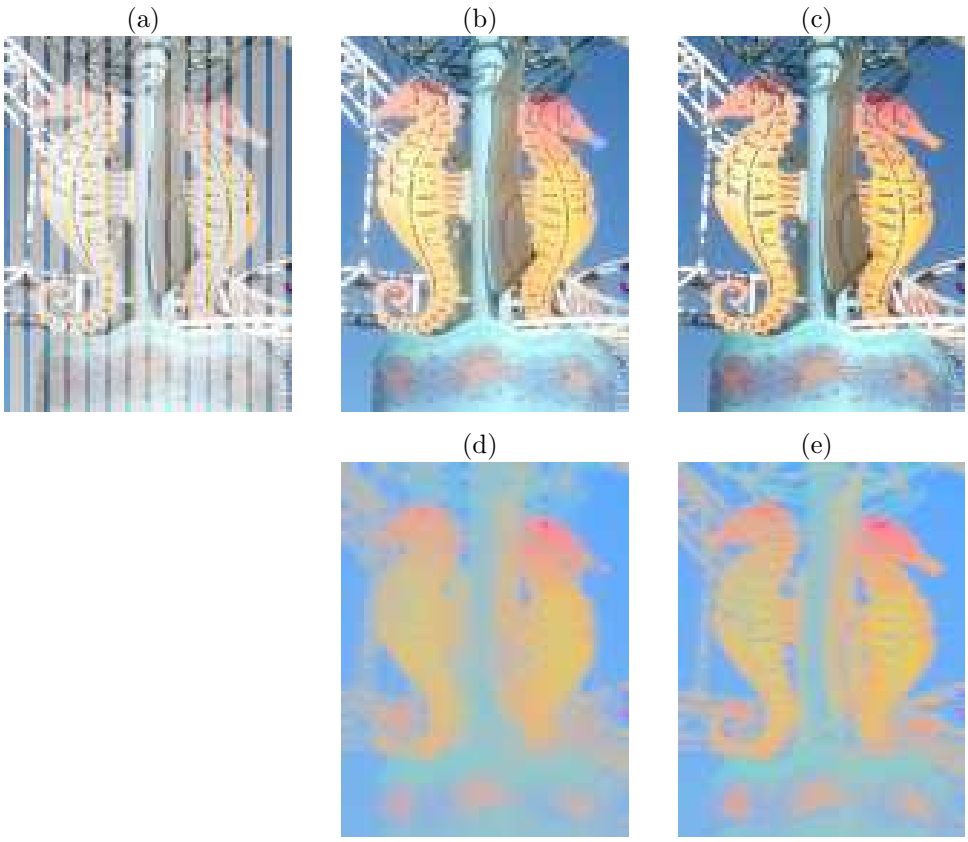

Figure 2: (a) The given image. Thin strips are where the colors are known. (b) TV colorized result. (c) The original image. The second row shows the corresponding chromaticity for each image. The seahorses as well as the base have multiple colors in each region, and image has many details. However, the image is colorized close to the original image.

such that $u(x) \in S^2$ for a.e. $x \in \Omega$. We consider the following functional for colorization

$$F(C) = \int_\Omega g(|\nabla B|)|\nabla C|^2 dx + \lambda \int_{D^c} |C - C_o|^2 dx, \tag{6}$$

and the corresponding minimization problem

$$(\mathcal{P}) \qquad \min \left\{ F(C) : C \in W^{1,2}(\Omega; S^2) \right\}.$$

Here $g : \mathbb{R}^+ \to \mathbb{R}^+$ is a monotone decreasing function such that $g(0) = 1$, $g(t) > 0$ for any $t > 0$, and $\lim_{t \to +\infty} g(t) = 0$. Examples of the function g are

$$g(t) = \frac{1}{1 + (t/a)^2}, \qquad \text{or} \qquad g(t) = e^{-(t/a)^2}, \tag{7}$$

with $a > 0$. As in the previous section, $B_o(x) = |f_o(x)|$ denotes the brightness datum which is known everywhere in Ω. In the functional (6), B is a regularization of B_o since we assume $B_o \in L^\infty(\Omega)$, and we need the derivatives of the brightness function in the sequel. We define B by

$$B = G_\sigma * B_o, \qquad G_\sigma(x) = \frac{A}{\sigma} \exp\left(-\frac{|x|^2}{4\sigma} \right), \tag{8}$$

where $*$ denotes the convolution operator and A is a positive constant. We have $B \in \mathcal{C}^\infty(\overline{\Omega})$. (This is for theoretical purposes, and in the discrete case we may use B_o directly if noise on brightness data is negligible, see below.)

As in the previous section, we consider the penalized version of the variational problem for chromaticity S^2 fitting. For any real number $\alpha > 0$, we consider the functional

$$F_\alpha(C) = \int_\Omega g(|\nabla B|)|\nabla C|^2 dx + \lambda \int_{D^c} |C - C_o|^2 dx + \alpha \int_\Omega \left(1 - |C|\right)^2 dx, \tag{9}$$

and the corresponding minimization problem

$$(\mathcal{P}_\alpha) \qquad \min \left\{ F_\alpha(C) : C \in W^{1,2}(\Omega; \mathbb{R}^3),\ |C(x)| \leq 1 \text{ for a.e. } x \in \Omega \right\}.$$

Different from the TV colorization model considered in the previous section, the minimization of the functional F with respect to the chromaticity C is now affected by the brightness data B_o. The first term in the functional F is the functional of harmonic maps [19, 28] weighted by the function g. Harmonic maps have been used for color image processing in [42, 43]. The value of the function $g(|\nabla B|)$ is close to one in regions where B_o is slowly varying, while it is small at the edges of brightness, if both σ and the constant a in (7) are small enough. Hence, the first term of F acts as a regularization functional such that the diffusion of chromaticity is inhibited across the edges of B_o, yielding a sharp transition in the function C. The second term in the functional F again requires the unitary vector field C to be close to the chromaticity data C_o in D^c. Therefore, the minimizer is a piecewise smooth color field, which is smooth in regions where the brightness B_o is slowly varying. If C is a solution of $(\mathcal{P})$, the colorized image f can be again defined by setting $f = B_o C$.

The present model is related to Sapiro's model [39] in the sense that geometry of the color image is provided by the geometry of grayscale information. In our model, edge information is derived from brightness information. In principle, this model is also related to piecewise smooth Mumford-Shah segmentation [34], since our model yields smooth color for each homogeneous region, while edge information is enforced by the weight function $g(\nabla B)$.

The colorization model (9) is flexible for colorization. Since *(i)* it is less sensitive to the size of the inpainting domain (except for computation time) compared to TV colorization in previous section. The given color diffuses as long as it meets the boundary of region enforced by the brightness information. *(ii)* By using the chromaticity color model, natural color blending is possible with respect to geodesic direction in chromaticity space S^2. In a homogeneous region, if different colors are given, this model will naturally diffuse the color by diffusing the vector values in S^2 in geodesic direction between colors. In addition, *(iii)* by varying the edge function $g(\nabla B)$, this model can be extended to deal with colorization of noisy images or texture colorization. We further discuss the details of these extensions.

For gray images with noise, it is convenient to replace the convolution (8) with a selective smoothing in order to preserve the edges. For instance, the regularized Perona-Malik equation of [22] could be used:

$$\frac{\partial B}{\partial t} - \operatorname{div}\left(g(|\nabla G_\sigma * B|)\nabla B\right) = 0, \qquad B(x,0) = B_o(x). \tag{10}$$

The time variable t in the evolution equation corresponds to a spatial scale analogous to σ. By the regularity result in [22], we have $B(x,t) \in \mathcal{C}^\infty(\overline{\Omega})$ for any $t > 0$. Then the spatial gradient ∇B, evaluated at time t, can be used inside the g function in the functionals (6) and (9).

With wide range of recent image decomposition literature using G-norm, these techniques can be applied for texture colorization. In [33], Meyer introduced an image decomposition model based on the Rudin-Osher-Fatemi's total variation minimization (TV) model [37]. A given image I is separated into $I = u + v$ by minimizing the following functional,

$$\inf_{(u,v) \in BV \times G / I = u+v} \int_\Omega |Du| + \eta \|v\|_G \,, \tag{11}$$

where η is a positive weight. The first term is a TV minimization which reduces u as the BV component of the original image I. The second term gives the v component containing the oscillatory part of the image, which is textures and noise. A distribution v belongs to G if v can be written as

$$v = \partial_1\psi_1 + \partial_2\psi_2 = \mathrm{div}(\psi) \quad \psi_1, \psi_2 \in L^\infty(\Omega).$$

The G-norm $\|v\|_G$ in (11) is defined as the infimum of all $L^\infty(\Omega)$-norms of the functions $|\psi|$, where $v = \mathrm{div}(\psi)$. Any function belonging to the space G can present strong oscillations, nonetheless has a small norm [4, 33]. Meyer's model (11) has been studied and implemented by many researchers, and literature on image decomposition models can be found in [2, 3, 4, 17, 18, 32, 35, 41, 45, 47, 48]. For our application, we use approaches in [3, 5], minimizing a convex functional by considering its dual functional. We first decompose the image brightness B_o into two components $B_o = B_u + B_v$ where B_u is the BV component of the original image B_o, and B_v is the oscillatory part of image which represents noise or texture. Then, we minimize the functional (9) with $B = G_\sigma * B_u$.

In the following subsections, we give the convergence properties of minimizers of the penalized variational problems, and we present numerical experiments.

3.1 Convergence of minimizers for the functional with penalty term

The following proposition is analogous to Proposition 1 of Section 2.1.

Proposition 2 *For any $\alpha > 0$, there exists a solution to the variational problem $(\mathcal{P}_\alpha)$. Let $\{C_\alpha\}_\alpha \subset W^{1,2}(\Omega;\mathbb{R}^3)$ be a sequence of functions such that α tends to infinity and C_α solves the variational problem $(\mathcal{P}_\alpha)$ for any $\alpha > 0$. Then, there exist a function $C \in W^{1,2}(\Omega; S^2)$ and a subsequence $\{C_{\alpha_k}\}_k$ such that C_{α_k} converges strongly to C in $L^p(\Omega;\mathbb{R}^3)$ for all $1 \le p < \infty$ as k tends to infinity, and C solves the variational problem $(\mathcal{P})$.*

Proof. The proof is similar to that of Proposition 1, hence we sketch only the main points.

Because of the regularization, either (8) or (10), we have $B \in \mathcal{C}^\infty(\overline{\Omega})$, so that ∇B is bounded in the closure of Ω. Hence, by the properties of the function g it follows that there exists a constant $c > 0$ such that

$$g(|\nabla B(x)|) > c \quad \text{for any } x \in \Omega. \tag{12}$$

Then the functional F_α is coercive in $W^{1,2}(\Omega;\mathbb{R}^3)$, being $|C(x)| \le 1$ a.e. Since the integrand in the first term of F_α is a convex function of ∇C for every $x \in \Omega$, by standard properties of Sobolev spaces, the functional F_α is also lower semicontinuous. Then a solution of the variational problem $(\mathcal{P}_\alpha)$ exists for any $\alpha > 0$.

Let $\{C_\alpha\}_\alpha$ be a sequence such that C_α solves the variational problem $(\mathcal{P}_\alpha)$ for any $\alpha > 0$. There exists a positive constant L, independent of α, such that $F_\alpha(C_\alpha) \le L$ for any $\alpha > 0$. Then, using (12), we have

$$\int_\Omega |\nabla C_\alpha|^2 dx \le \frac{L}{c}, \qquad \|C_\alpha\|_{L^\infty(\Omega)} \le 1,$$

for any $\alpha > 0$. Then, by the compactness properties of Sobolev spaces, there exist a function $C \in W^{1,2}(\Omega;\mathbb{R}^3)$ such that $|C(x)| \le 1$ for a.e. $x \in \Omega$, and a subsequence $\{C_{\alpha_k}\}_k$ such that C_{α_k} converges to C a.e. in Ω, and strongly in $L^p(\Omega;\mathbb{R}^3)$ for all $1 \le p < +\infty$, as k tends to infinity. Therefore, $|C_\alpha|$ converges to one in $L^2(\Omega)$, and $|C(x)| = 1$ for a.e. $x \in \Omega$, so that $C \in W^{1,2}(\Omega; S^2)$.

Let now $\widehat{C} \in W^{1,2}(\Omega; S^2)$; since $|\widehat{C}(x)| = 1$ for a.e. $x \in \Omega$, we have $F(\widehat{C}) \ge F_\alpha(C_\alpha)$ for any $\alpha > 0$. Then, by lower semicontinuity, it follows

$$\begin{aligned} F(\widehat{C}) &\ge \liminf_{k\to+\infty} F_{\alpha_k}(C_{\alpha_k}) \ge \liminf_{k\to+\infty} \int_\Omega g(|\nabla B|)|\nabla C_{\alpha_k}|^2 dx + \liminf_{k\to+\infty} \lambda \int_{D^c} |C_{\alpha_k} - C_o|^2 dx \\ &\ge \int_\Omega g(|\nabla B|)|\nabla C|^2 dx + \lambda \int_{D^c} |C - C_o|^2 dx = F(C). \end{aligned}$$

Since this inequality holds for any $\widehat{C} \in W^{1,2}(\Omega; S^2)$, it follows that C solves the problem $(\mathcal{P})$. $\square$

We conclude this subsection by noting that instead of the penalty term used in the functional (9), one can also consider the term

$$\alpha \int_\Omega \left(1 - |C|^2\right)^2 dx,$$

which corresponds to the Ginzburg-Landau functional [20, 21].

3.2 Numerical experiments for colorization via weighted harmonic map

For numerical computation, we solve the Euler-Lagrange equation of the functional (9) by means of a time marching method,

$$C_t = \nabla \left(g(|\nabla B|)\, \nabla C\right) - \widehat{\lambda}(C - C_o) - \alpha \left(1 - \frac{1}{|C|}\right) C. \tag{13}$$

Here $\widehat{\lambda}$ includes a characteristic function indicating the region for inpainting as in the previous section. The function g of exponential type (7) has been used in the experiments. For discretization, simple forward differencing for first derivatives and central differencing for second order derivatives are used. The regularization by means of convolution (8) has been introduced in the previous section for the purpose of mathematical analysis, i.e. to define the gradient ∇B and to make the functionals F, F_α coercive in the Sobolev space $W^{1,2}$. In the discrete setting, the derivatives of the data B_o are always defined by means of finite differences. Therefore, convolution can be avoided for images with negligible noise, and it was unnecessary for the computer experiments here presented.

The algorithm goes as follows:

1. From an image f_o given in D^c, chromaticity C_o is separated, i.e. $C_o = \dfrac{f_o}{|f_o|}$.

2. Then C is iterated with the time marching (13). (In theory, after each iteration, C is projected to be $|C(x)| \leq 1$. In our experiment, with large α values, this was not necessary.)

3. The reconstructed image is computed from $f = CB_o$.

For our experiments, the image f is in between $[0, 1]$, and $\alpha = 10$ and $\lambda = 10$.

Figure 3 and Figure 4 show numerical results using colorization via weighted harmonic map. From small patches of colors, colors are reconstructed through out the image well preserving the edge information. The recovered colors are close to the original clean images. In Figure 4, very small areas of colors are given (about 11.7%) . Nevertheless, the algorithm recovers more than half of colors successfully and stops at definite boundaries. The peppers in the right side of images clearly stay gray color, since there is no color information given. When more color patches are given, the algorithm colorizes them successfully.

Figure 5 shows an experiment with natural color blending. Notice that two thin strips (only 6.7% total) of colors are given, which are two different colors. Then, $\int g\, |\nabla C|^2 dx$ term diffuses the two colors within one region and naturally blends the two colors. Color blend is achieved in geodesic directions in chromaticity space. Compared to original image, the details of varying colors are lost in the middle, however, the method gives a reasonable colorization result.

Figure 6 and Figure 7 show an example of texture image colorization. The given brightness image B_o is first decomposed into BV part B_u and texture B_v, then equation (13) with B_u instead of B_o is applied. The following is a brief description of how to compute B_u from B_o, details can be found at [3, 4, 5].

Algorithm for Image Decomposition

1. Initially we set, $B_u = B_o$ and $B_v = 0$.

2. Fix B_v, then solve for B_u by

$$\frac{B_u^{n+1} - B_u^n}{\Delta t} = \nabla \cdot \frac{\nabla B_u^n}{|\nabla B_u^n|} + \nu(B_o - B_u^n - B_v).$$

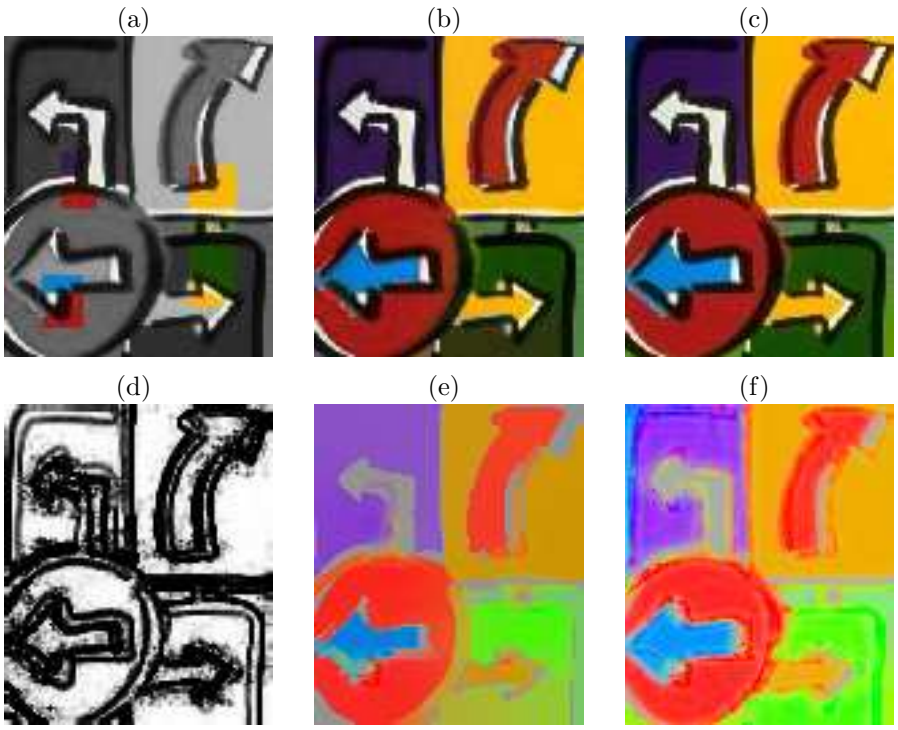

Figure 3: (a) The given image. (b) Colorization result by weighted harmonic map. (c) The original image. (d) The plot of $g(|\nabla B_o|)$. (e) Chromaticity of colorization result. (f) Chromaticity of original image. From small given color patches, the whole image is successfully colorized.

3. $B_w = B_o - B_u - B_v$.
4. Fix B_u, and solve for B_w by
$$\frac{B_w^{n+1} - B_w^n}{\Delta t} = \nabla \cdot \frac{\nabla B_w^n}{|\nabla B_w^n|} + \mu(B_o - B_u^{n+1} - B_w^n).$$
5. Update $B_v^{n+1} = B_o - B_u - B_w$.

For our application, we only utilize B_u. These two total variation equations are solved by digital TV filter [13]. The parameter ν is similar to the fitting parameter of TV denoising [37], and μ represents amount of detail to keep for B_v. For experiments, we use $\nu = 0.5$ and $\mu = 100$.

Figure 6 shows comparison between original image and colorized result, and chromaticity is shown. In the result, since original color of right eye is not given, it stays gray color, while other areas are colorized clearly and close to original image. Figure 7 shows the difference between using image decomposition for texture removal $g(|\nabla B_u|)$ versus using simple brightness information $g(|\nabla B_o|)$. Due to highly oscillating texture, the colorization algorithm does not diffuse color beyond each small region, while texture decomposition reasonably colorizes the image without getting stuck at fine details. Notice the difference between the values $g(|\nabla B_u|)$ and $g(|\nabla B_o|)$.

4 Conclusion

We explored variational colorization models: TV colorization and colorization via weighted harmonic map. Calculus of variations provides flexibility in modeling, and mathematical analysis yields a sound basis for the

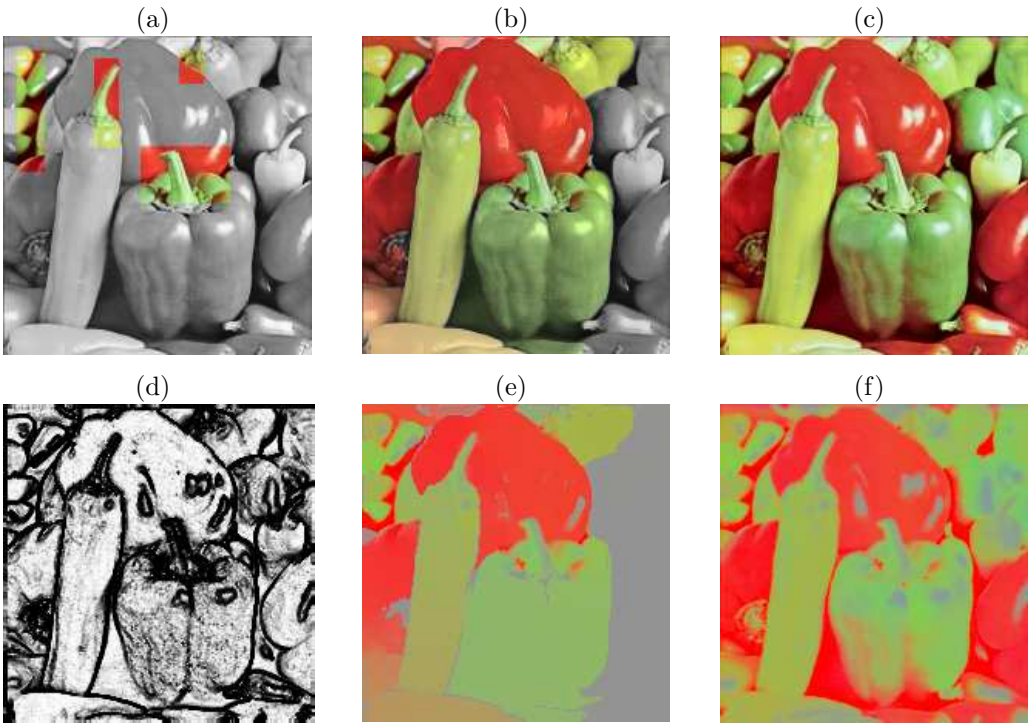

Figure 4: (a) The given image. (b) Colorization result by weighted harmonic map. (c) The original image.(d) The plot of $g(|\nabla B_o|)$. (e) Chromaticity of colorization result. (f) Chromaticity of original image. The regions without any color information stay gray values, while places with given color are colorized by diffusion of the given color. From very small color patches, more than half of image is colorized successfully.

models. By using chromaticity and brightness color model, chrominance is accurately modeled. We consider a penalized version of the variational problems in order to handle the nonconvex constraint $|C(x)| = 1$. We discuss the consistency of such models by proving existence and convergence of minimizers of the functionals with penalty term to minimizers for the ideal model. Numerical results are shown to validate the model.

Numerical implementation shows effectiveness of TV colorization. Complicated details can be recovered with simple calculation given reasonable chrominance information. The weighted harmonic map model can deal with bigger colorization area. With only small area of color given, color can be diffused to large region. With this model, color blending is naturally achieved by geodesic direction in chromaticity space, and it can deal with texture colorization combined with image decomposition methods.

Acknowledgment

Both authors acknowledge IMA for their valuable support. During long term visit to IMA during the Thematic year on Imaging, this collaboration started and developed. Both authors would like to thank IMA for supporting their visit.

References

[1] L. Ambrosio, N. Fusco, and D. Pallara. *Functions of bounded variations and free discontinuity problems.* Oxford mathematical monographs. Oxford University Press, 2000.

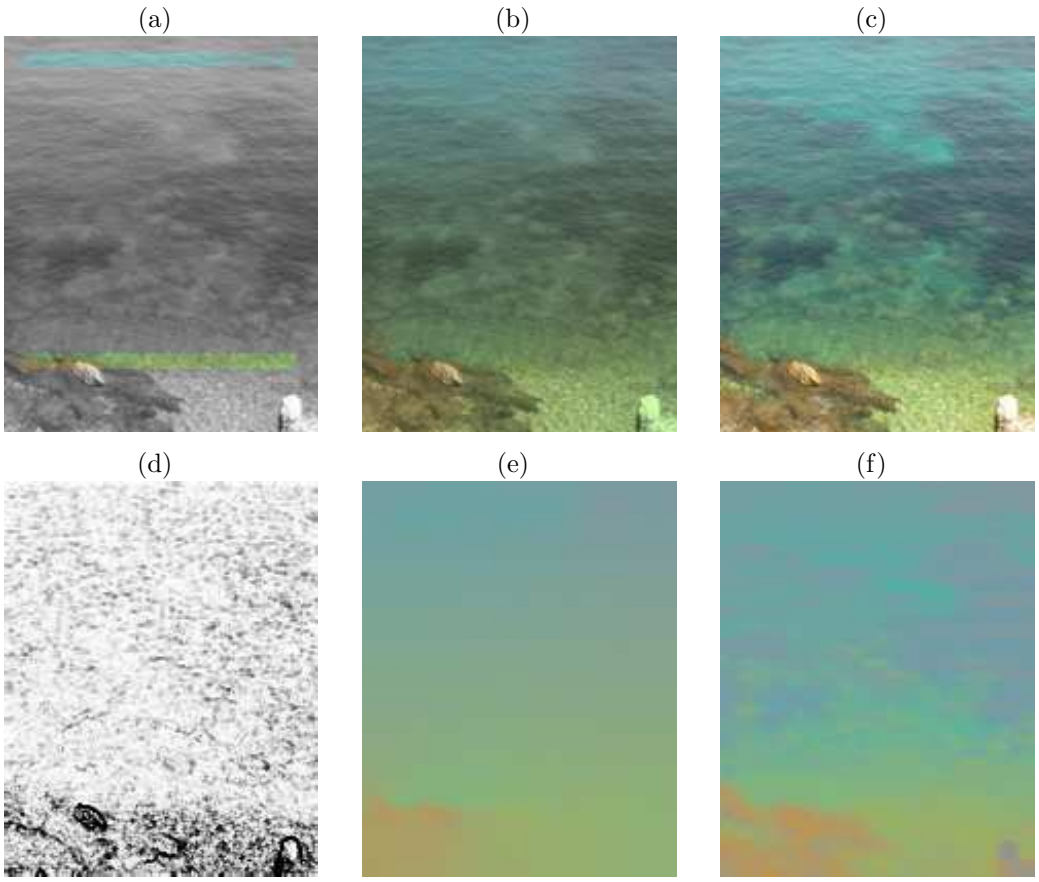

Figure 5: (a) The given image. (b) Colorization result by weighted harmonic map. (c) The original image. (d) The plot of $g(|\nabla B_o|)$. (e) Chromaticity of colorization result. (f) Chromaticity of original image. Two thin strips of different colors are given fairly apart from each other in one large region in image (a), and color blending is naturally achieved in chromaticity space.

[2] G. Aubert and J-F. Aujol. Modeling very oscillating signals. Application to image processing. *Applied Mathematics and Optimization*, 51(2):163–182, 2005.

[3] J-F. Aujol, G. Aubert, L. Blanc-Féraud, and A. Chambolle. Image decomposition into a bounded variation component and an oscillating component. *Journal of Mathematical Imaging and Vision*, 22(1), January 2005.

[4] J-F. Aujol and A. Chambolle. Dual norms and image decomposition models. *International Journal of Computational Vision*, 63(1):85–104, 2005.

[5] J-F. Aujol and S. H. Kang. Color image decomposition and restoration. *Journal of Visual Communication and Image Representation*, 17(4):916–928, 2006.

[6] C. Ballester, M. Bertalmio, V. Caselles, G. Sapiro, and J. Vergera. Filling-in by joint interpolation of vector fields and gray levels. *IEEE Trans. Image Processing*, 10(8):1200–1211, 2001.

[7] M. Bertalmio, G. Sapiro, V. Caselles, and C. Balleste. Image inpainting. *Proceedings of SIGGRAPH 2000, New Orleans*, 2000.

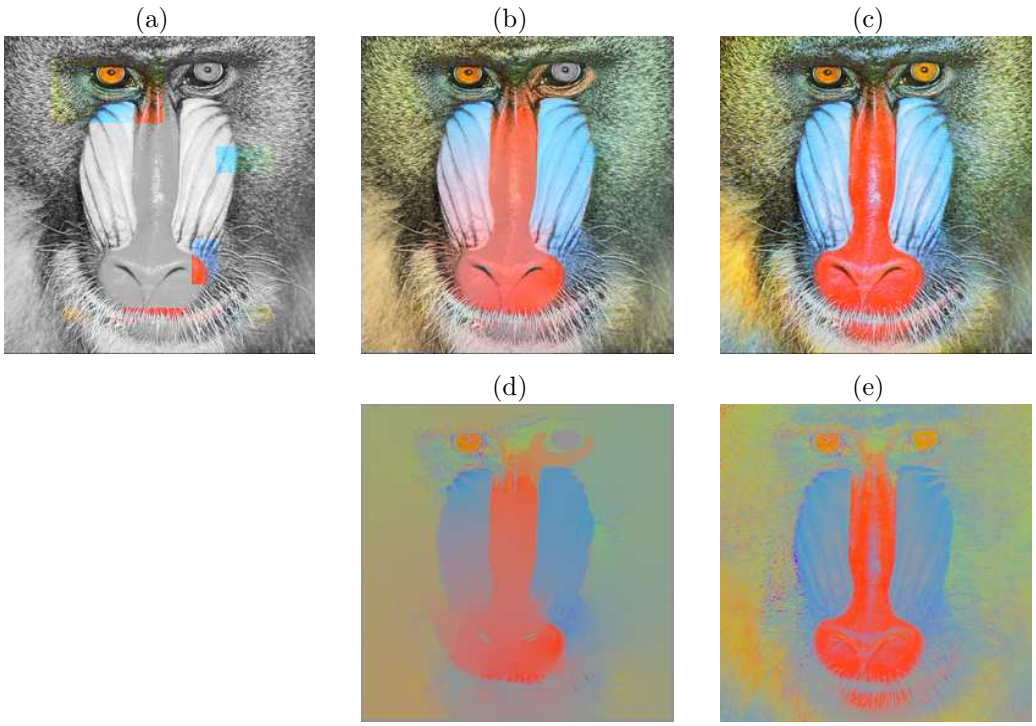

Figure 6: (a) The given image. (b) The texture colorization result. Weighted harmonic map colorization with image decomposition for brightness value. (c) The original image. Second row images show the chromaticity of each image.

[8] P. Blomgren and T. F. Chan. Color TV: Total variation methods for restoration of vector-valued images. *IEEE Trans. Image Process.*, 7(3):304–309, 1998.

[9] V. Caselles, B. Coll, and J. Morel. Geometry and color in natural images. *Journal of Mathematical Imaging and Vision*, 16(2):89–105, 2002.

[10] T. F. Chan and S. H. Kang. Error analysis for image inpainting. *Journal of Mathematical Imaging and Vision*, 2006.

[11] T. F. Chan, S. H. Kang, and J. Shen. Total variation denoising and enhancement of color images based on the CB and HSV color models. *J. Visual Comm. Image Rep.*, 12(4):422–435, 2001.

[12] T. F. Chan, S. H. Kang, and J. Shen. Euler's elastica and curvature based inpainting. *SIAM Journal of Applied Math.*, 63(2):564–592, 2002.

[13] T. F. Chan, S. Osher, and J. Shen. The digital TV filter and non-linear denoising. *IEEE Trans. Image Process.*, 10(2):231–241, 2001.

[14] T. F. Chan and J. Shen. Mathematical models for local deterministic inpaintings. *SIAM Journal of Applied Math.*, 62(3):1019–1043, 2001.

[15] T. F. Chan and J. Shen. Non-Texture inpainting by curvature-driven diffusion (CDD). *Journal of Visual Comm. and Image Rep.*, 12(4):436–449, 2001.

[16] T. Chen, Y. Wang, V. Schillings, and C. Meinel. Grayscale image matting and colorization. *In Proceedings of Asian Conference on Computer Vision (ACCV)*, 2004.

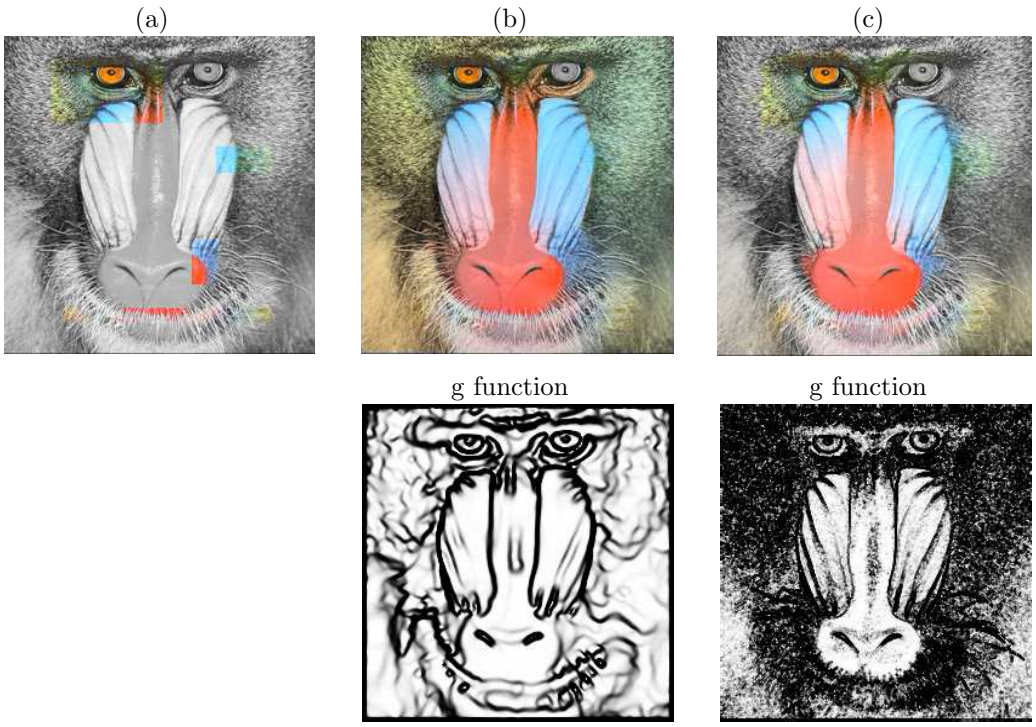

Figure 7: (a) The given image. (b) The texture colorization result. (c) Colorization by using simple brightness information. (d) The plot of $g(|\nabla B_u|)$. (e) The plot of $g(|\nabla B_o|)$. Notice the difference between the values of $g(|\nabla B_u|)$ and $g(|\nabla B_o|)$, and its effects in the results.

[17] G. Chung, T. Le, L. H. Lieu, N. Tanushev, and L. Vese. Computational methods for image restoration, image segmentation, and texture modeling, computational imaging iv. *Proc. of SPIE-IS&T Electronic Imaging*, 6065:60650J–1 – 60650J–15, 2006.

[18] I. Daubechies and G. Teschke. Variational image restoration by means of wavelets: simultaneous decomposition, deblurring and denoising, 2005.

[19] J. Eells and J.H. Sampson. Harmonic mappings of riemannian manifolds. *Amer. J. Math*, 86:109–160, 1964.

[20] H. Brezis F. Bethuel and F. Helein. Singular limit for the minimization of ginzburg-landau functionals. *C.R. Acad. Sci. Paris Ser. I Math.*, 314:891–895, 1992.

[21] H. Brezis F. Bethuel and F. Helein. Asymptotics for the minimization of a ginzburg-landau functional. *Calc. Var. Partial Diff. Equat.*, 1:123–148, 1993.

[22] J.M. Morel F. Catté, P.L. Lions and T. Coll. Image selective smoothing and edge detection by nonlinear diffusion. *SIAM J. Numer. Anal.*, 29(1):182–193, 1992.

[23] M. Fornasier. Nonlinear projection digital image inpainting and restoration methods. *Journal of Mathematical Imaging and Vision*, 24(3):359 – 373, 2006.

[24] M. Fornasier and R. March. Restoration of color images by vector valued BV functions and variational calculus. *preprint (http://www.iac.cnr.it/∼march/)*, 2006.

[25] M. Giaquinta, G. Modica, and J. Soucek. Variational problems for maps of bounded variation with values in S^1. *Calculus of Variations and Partial Differential Equations*, 1(1):87–121, 1993.

[26] E. Giusti. *Minimal surfaces and functions of bounded variation*, volume 80 of *Monographs in Mathematics*. Birkhäuser, 1984.

[27] R. Gonzalez and R. Wood. *Digital Image Processing*. Addison-Wesley, 1992.

[28] J.M. Coron H. Brezis and E.H. Lieb. Harmonic maps with defects. *Comm. Math. Phys.*, 107:649–705, 1986.

[29] R. Irony, D. Cohen-Or, and D. Lischinski. Colorization by example. *Proceedings of Eurographics Symposium on Rendering*, pages 201–210, 2005.

[30] R. Kimmel and N. Sochen. Orientation diffusion or how to comb a porcupine ? *J. Visual Comm. and Image Rep.*, 13:238–248, 2001.

[31] A. Levin, D. Lischinski, and Y. Weiss. Colorization using optimization. *Proceedings of the 2004 SIGGRAPH Conference*, 23(3):689–694, 2004.

[32] S. Levine. An adaptive variational model for image decomposition. *Energy Minimization Methods in Computer Vision and Pattern Recognition, Springer Verlag LCNS*, (3757):382–397, 2005.

[33] Y. Meyer. *Oscillating Patterns in Image Processing and Nonlinear Evolution Equations: The Fifteenth Dean Jacqueline B. Lewis Memorial Lectures*, volume 22 of *University Lecture Series*. AMS, Providence, 2001.

[34] D. Mumford and J. Shah. Optimal approximations by piecewise smooth functions and associated variational problems. *Comm. Pure Appl. Math.*, 42(5):577–685, 1989.

[35] S. Osher, A. Sole, and L. Vese. Image decomposition and restoration using total variation minimization and the H^{-1} norm. *SIAM multiscale Model. Simul.*, 1(3):349–370, 2003.

[36] P. Perona. Orientation diffusion. *IEEE Trans. Image Process.*, 7(3):457–467, 1998.

[37] L. Rudin, S. Osher, and E. Fatemi. Nonlinear total variation based noise removal algorithms. *Physica D*, 60:259–268, 1992.

[38] D. Sýkora, J. Buriánek, and J. Žáta. Unsupervised colorization of black-and-white cartoons. *Proceedings of the 3rd international symposium on Non-photorealistic animation and rendering(ACM)*, pages 121 – 127, 2004.

[39] G. Sapiro. Inpainting the colors. *ICIP 2005. IEEE International Conference on Image Processing*, 2:698–701, 2005.

[40] G. Sapiro and D. Ringach. Anisotropic diffusion of multivalued images with applications to color filtering. *IEEE Trans. Image Process.*, 5:1582–1586, 1996.

[41] J.L. Starck, M. ELad, and D.L. Donoho. Image decomposition: separation of texture from piecewise smooth content, 2003. Wavelets: Applications in Signal and Image Processing X.

[42] B. Tang, G. Sapiro, and V. Caselles. Diffusion of general data on non-flat manifolds via harmonic maps theory: the direction diffusion case. *Int. J. Computer Vision*, 36:149–161, 2000.

[43] B. Tang, G. Sapiro, and V. Caselles. Color image enhancement via chromaticity diffusion. *IEEE Trans. Image Process.*, 10:701–707, 2001.

[44] P. E. Trahanias, D. Karako, and A. N. Venetsanopoulos. Directional processing of color images: theory and experimental results. *IEEE Trans. Image Process.*, 5(6):868–880, 1996.

[45] L. Vese and T. Le. Decomposition of images into cartoon and texture using the total variation and div(bmo). *SIAM Multiscale Modeling and Simulation*, 4(2):309–423, 2005.

[46] L. Vese and S. Osher. Numerical methods for p-harmonic flows and applications to image processing. *SIAM J. Numer. Anal.*, 40(6):2085–2104, 2002.

[47] L. Vese and S. Osher. Modeling textures with total variation minimization and oscillating patterns in image processing. *Journal of Scientific Computing*, 19(1-3):553–572, 2003.

[48] L. Vese and S. Osher. Image denoising and decomposition with total variation minimization and oscillatory functions. *Journal of Mathematical Imaging and Vision*, 20:7–18, 2004.

[49] L. Yatziv and G. Sapiro. Fast image and video colorization using chrominance blending. *IEEE Transactions on Image Processing*, 15(5):1120–1129, 2006.